Original scientific paper
https://doi.org/10.33180/InfMIDEM2023.301

Informacije MIDEM
Journal of Microelectronics,
Electronic Components and Materials
Vol. 53, No. 3(2023), 121 – 135

Existence of Capacitive Effects in a Tungsten-based SDC Memristive System

Ceylan Dalmış[1], Reşat Mutlu[1], Ertuğrul Karakulak[2]

[1]Department of Electronics and Communication Engineering, Çorlu Engineering Faculty, Tekirdağ Namık Kemal University, Çorlu, Tekirdağ, Turkey
[2]Electronics Department, School of Vocational and Technical Sciences, Tekirdağ Namık Kemal University, Tekirdağ, Turkey

Abstract: Following the discovery of a thin-film memristive system behaving as a memristor in 2008, memcapacitor and memcapacitive systems have also been described and become hot research areas. Tungsten-based SDC (Self-Directed Channel) memristors are already in the market and have already been used in circuit applications. They are modeled with the mean metastable switch memristor model in the literature. A memristor must have the three fingerprints described by Chua et al. In this paper, it is shown that the behavior of the Tungsten-based memristors is more complex than a memristive system and they do not always meet the three fingerprints of the memristor. It has been experimentally found that the capacitive effects are dominant at low frequencies when it is excited with a square wave voltage source when the Tungsten-based memristor is connected in series with a capacitor. It is important to model the new circuit element memristor accurately. "The Tungsten-based memristors" cannot be modeled just as a memristive system and only with the mean metastable switch memristor model. It is suggested that, perhaps, it can be modeled considering memcapacitive effects.

Keywords: memristor, memristive systems, zero-crossing hysteresis curve, memcapacitive effects, memcapacitor

Obstoj kapacitivnih učinkov v memristivnem sistemu SDC na osnovi volframa

Izvleček: Potem ko je bil leta 2008 odkrit memristivni sistem s tanko plastjo, ki se obnaša kot memristor, so bili opisani tudi kondenzatorji in memkapacitivni sistemi. Memristorji SDC (Self-Directed Channel) na osnovi volframa se že uporabljajo v komercialnih vezjih. V literaturi so modelirani z modelom srednjega metastabilnega stikala memristorja. Memristor mora imeti tri prstne odtise, ki so jih opisali Chua et al. V članku je prikazano, da je obnašanje memristorjev na osnovi volframa bolj zapleteno kot memristivni sistem in ne izpolnjujejo vedno treh prstnih odtisov memristorja. Eksperimentalno je bilo ugotovljeno, da pri nizkih frekvencah prevladujejo kapacitivni učinki, ko je memristor na osnovi volframa vzbujen z napetostnim virom s kvadratnim valovanjem in je zaporedno povezan s kondenzatorjem. Pomembno je, da se novi element vezja memristor natančno modelira. „Memristorjev na osnovi volframa" ni mogoče modelirati samo kot memristivni sistem in samo z modelom srednjega metastabilnega stikala memristorja. Predlagano je, da ga je morda mogoče modelirati ob upoštevanju memkapacitivnih učinkov.

Ključne besede: memristor, memristivni sistemi, krivulja histereze z ničelnim prehodom, memkapacitivni učinki, mem-kondenzator

** Corresponding Author's e-mail: email@server.com, email2@server.com*

1 Introduction

Memristor was claimed as a missing nonlinear fundamental circuit element in 1971 [1]. In 1976, it was shown that there were systems with similar properties to memristors and they are called memristive systems [2]. A thin-film TiO_2 memristive system was shown to behave as a memristor in 2008 [3]. Memristor is a highly nonlinear circuit element, and its electromagnetic theory is elusive unlike other circuit elements [4]. It has emerged as a popular nonlinear circuit element in the last two decades [5]. The memristive effects are quite common in nano dimensions [6, 7]. Some memristor research has focused on finding new materials behaving as memristors [6, 7]. Resistive RAMs are also

How to cite:
C. Dalmış et al., "Existence of Capacitive Effects in a Tungsten-based SDC Memristive System", Inf. Midem-J. Microelectron. Electron. Compon. Mater., Vol. 53, No. 3(2023), pp. 121–135

regarded as memristors [8]. Memristors may cause new analog and digital circuit applications to be found [5, 9]. Programmable circuit applications of the memristor are also promising [10, 11]. An ideal memristor has not been found yet [12]. Nowadays, memristive systems are also called memristors [12]. An ideal memristor must have a zero-crossing hysteresis curve [2]. The three fingerprints of memristors are commonly used to identify them [13]. Some memristor research focused on modeling nonlinear dopant drift memristors with window functions [14-20]. Such memristor models possess the three fingerprints of memristors.

A memcapacitor is a flux-dependent capacitor and a memcapacitive system is a system with similar properties to memcapacitors [6, 21]. An ideal memcapacitor or a memcapacitive system is also a nonlinear circuit element [21]. An ideal memcapacitor's charge-voltage characteristic or hysteresis loop is also frequency-dependent [21, 22]. The memcapacitive effects are also common in the literature [6, 23, 24]. The capacitance of some memcapacitive systems may be negative [25]. Memcapacitive effects can also be found in nanopores [26]. Solid-state memcapacitors can be used to make circuits that cannot be made with LTI capacitors [27]. Memcapacitive effects are shown to exist in an HP TiO_2 memristor [28]. An Au/Ti–HfO2-InP/InGaAs diode needs both memristive and memcapacitive effects to be modeled correctly [29]. A memcapacitor device showing chaotic behavior is described in [30]. Memcapacitors can be used in oscillator circuits [31-32]. There are already memcapacitor-based chaotic oscillators made in the literature [33-35]. In opposite to memristors, memcapacitors store energy and their charging efficiency can be polarity-dependent [36]. Memcapacitors can also be used for computing [37].

The market has already seen the emergence of Carbon- and Tungsten-based memristors [38]. They are also reported to have zero-crossing hysteresis curves [38] and have already been used in chaotic circuits and for educational purposes [39-40]. They are suggested for use in a machine-learning circuit [41]. The usage of Knowm memristors in threshold logic circuits is examined in [42]. These memristors are suggested to be used with a series protection resistor [38]. According to [1], the equivalent circuit of a memristor connected in series with a resistor is also a memristor. That's why a Knowm memristor with a protection resistor is also a memristor. The Mean Metastable Switch Memristor Model (MMSMM) is presented for Tungsten-based Knowm memristors in [43]. In [44], the model is modified to include chaotic dynamics. The model in [43-44] gives a zero-crossing hysteresis curve. The models in [43-44] should be able to predict the waveforms of the circuits in which the Tungsten-based memristors are used.

A memristor-capacitor circuit can be found in a programmable filter [11]. A memristor-capacitor discharge circuit is examined in [14]. HP memristor-capacitor series circuit under DC excitation is examined analytically in [45]. In [46], it is shown that the Lambert W function can be used to analyze the charging and discharging of memristor-capacitor circuits. An analytical and experimental examination of a parallel memristor-capacitor circuit is made using the memristor's flux-charge characteristic [47]. To the best of our knowledge, the charging and discharging of the Tungsten-based memristor-capacitor circuit have not been examined experimentally. In this paper, we report the experimental results that were observed while examining a Tungsten-based memristor-capacitor-protection resistor (M-C-R_s) series circuit excited with a square wave signal, it has been found that the Tungsten-based memristors exhibit a non-zero crossing hysteresis curve, it is interesting that the same memristor has a zero-crossing hysteresis curve when excited with a sinusoidal wave or even a square wave, and this means that hysteresis behavior of a Tungsten-based memristor may not have zero-crossing hysteresis curve depending on its usage with other circuits. The implications of the experimental results are also discussed. This study is important because there is no other study in the literature examining the effect of the polarity of the memristor on the charging of the capacitor in an M-C-R_s circuit experimentally.

The paper is arranged as follows. The memristive and memcapacitive systems are briefly introduced in the second section. Information on a Tungsten-based Self-Directed Channel Memristor is given in the third section. Experimental results are given in the fourth section. The experimental results are discussed in the fifth section. The last section concludes the paper.

2 Memristive and memcapacitive systems

In this section, the memristive and memcapacitive systems are briefly explained.

2.1 Memristor and memristive systems

Memristive systems can be classified as either current-controlled or voltage-controlled. In [21], Ventra et al. have described an n^{th} degree voltage-controlled memristive system as

$$i(t) = G\left(x(t), v(t), t\right).v(t) \tag{1}$$

$$\frac{dx}{dt} = f\left(x(t), v(t), \mathrm{t}\right) \tag{2}$$

where $v(t)$, $i(t)$, and $G(x(t), v(t), t)$ are the voltage, the current, and the electrical conductance or the memductance of the memristive system, respectively, and $x(t)$ is the set of n state variables describing the internal state of the memristive system, that may be dependent on $v(t)$ and $x(t)$.

If ($x(t)$ is the flux of the system and its memductance is only dependent on it, the system describes an ideal memristor [2, 21]. The memristor symbol, which is defined in [1] and shown in Figure 1.a, is nowadays used for both memristors and memristive systems.

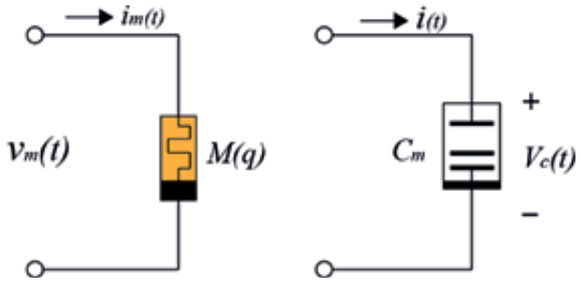

(a) b)

Figure 1: a) Memristor and b) Memcapacitor symbols.

For a memristor, the memductance must be always positive:

$$0 < G\left(x(t), \mathrm{v}(\mathrm{t}), t\right) < \infty \tag{3}$$

A memristor cannot store energy and it is a power-dissipating circuit element [1]. Memristive systems also dissipate power and do not store energy.

$$p(t) = v(t)\, i(t) \geq 0 \tag{4}$$

Under AC excitation, a memristor or a memristive system must have a zero-crossing hysteresis loop that has been first described in [2]. In [13], the claim has been made that all memristors or memristive systems must have the three fingerprints. They are given as:

- A memristor's current and voltage must be both zero at the same time or it must have a zero-crossing hysteresis loop under AC excitation.
- The hysteresis loop must be frequency-dependent, i.e., its shape varies with frequency. Its area decreases when frequency increases.
- The hysteresis loop converges to a single value function when the frequency becomes very high.

2.2 Memcapacitive systems

Some nonlinear capacitors obey the memcapacitive system definition [21]. Ventra et al. have described a voltage-controlled memcapacitive system as

$$q(t) = C\left(x, v_c, t\right) v_c(t) \tag{5}$$

$$\frac{dx}{dt} = f\left(x(t), \mathrm{v}(\mathrm{t}), \mathrm{t}\right) \tag{6}$$

where $q(t)$, $v_c(t)$, and $C(x, v_c, t)$ are the charge, the voltage, and the nonlinear capacitance (memcapacitance) of the memcapacitive system, respectively, and $x(t)$ is the set of n state variables describing the internal state of the memcapacitive system, that may be dependent on $v_c(t)$ and $x(t)$.

If $x(t)$ is the flux of a memcapacitive system and equal to the integral of its voltage with respect to time, the system describes an ideal memcapacitor, i.e., a memcapacitor is a special case of a memcapacitive system [21]. The memcapacitor symbol, which is defined in [21] and shown in Figure 1.b, is nowadays used for both memcapacitors and memcapacitive systems.

If there is only one state variable, the current of a memcapacitive system can be calculated as

$$i_c(t) = \frac{dq_c(t)}{\mathrm{dt}} = \frac{d\left(C\left(x(t), v_c(t), t\right) v_c(t)\right)}{\mathrm{dt}} = \frac{d\left(C\left(x(t), v_c(t), t\right)\right)}{\mathrm{dx}} \frac{dx}{\mathrm{dt}} v_c(t) + C\left(x(t), v_c(t), t\right) \frac{dv_c(t)}{\mathrm{dt}} \tag{7}$$

$$i_c(t) = \frac{d\left(C\left(x, v_c(t), t\right)\right)}{\mathrm{dx}} f\left(x(t), v(t), t\right) v_c(t) + C\left(x, v_c(t), t\right) \frac{dv_c(t)}{\mathrm{dt}} \tag{8}$$

2.3 Mean metastable switch memristor model

The Tungsten-based Knowm memristor symbol and the equivalent circuit of the MMSMM model are shown in Figure 2. A Tungsten-based Knowm memristor is modeled as a Schottky diode connected in parallel with a memristor or a memristive system, and Φ is a parameter that determines the contributions of these parallel connected circuit elements. The mean metastable switch memristor model (MMSMM) of a Tungsten-based Knowm memristor [43] is given as

$$i(t) = \left(\frac{\phi x}{R_{ON}} + \frac{\phi(1-x)}{R_{OFF}}\right) v(t) + (1-\Phi)\alpha\left(e^{\beta_1 v(t)} - e^{-\beta_2 v(t)}\right) \tag{9}$$

$$\frac{dx}{dt} = \frac{1}{\tau}\left(\frac{1}{1+e^{-\beta(v-V_{ON})}}(1-x) - \left(1 - \frac{1}{1+e^{-\beta(v+V_{OFF})}}\right)x\right) \tag{10}$$

Where $v(t)$ and $i(t)$ are the voltage and current of the Tungsten-based memristor, $x(t)$ is the state variable of the Tungsten-based memristor, R_{ON} and R_{OFF} are the minimum and maximum memristance of the memristive memory element shown in Figure 2, α, β_1, and β_2 are Schottky parameters, τ is a time constant that defines the rate of change of the state variable, V_{ON} is the positive threshold voltage, V_{OFF} is the negative threshold voltage, β is a temperature dependent parameter, reciprocal to thermal voltage, V_T, and equal to

$$\beta = \frac{1}{V_T} = \frac{e}{kT} \tag{11}$$

Where k is the Boltzmann constant, e is the electron charge, and T is the absolute temperature.

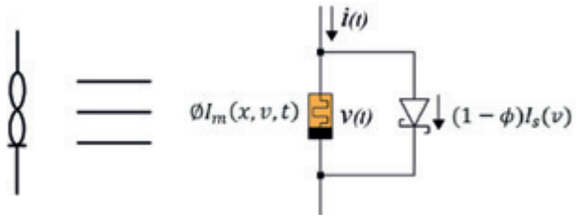

Figure 2: The equivalent circuit of a Tungsten-based Knowm memristor [43].

The state variable $x(t)$ ranges from 0 to 1. Tungsten-based memristor current considering the equivalent circuit shown in Figure 2 is given as

$$i(t) = \Phi I_m(x,v,t) + (1-\phi) I_s(v) \tag{12}$$

Where $I_m(x, v, t)$ is the current of an ideal memristor and $I_s(v)$ is the current of an ideal Schottky diode.

Φ is a positive parameter between zero and one. If Φ=1, the Schottky diode current is zero, and the equivalent circuit in Figure 2 turns into an ideal memristor. If Φ=0, the equivalent circuit in Figure 2 turns into a Schottky diode.

In [44], the threshold of the memristor is given as

$$V_{ON} = \frac{0,1cos\left(\left(4\pi\sqrt{x}\right)/\left(1,7-x\right)\right)}{1+10\sqrt{x}} + 0.14 \tag{13}$$

The chaotic memristor model given in [44] was not used in this study since the memristor was not examined at above the threshold voltages.

Considering Eq.s (9) and (10) and the three fingerprints of a memristor, the current and voltage of a Tungsten-based memristor must become zero at the same time since the MMSMM model also obeys memristive system equations.

3 Tungsten-based self-directed channel (SDC) memristor

The Self-Directed Channel (SDC) Tungsten-based Knowm memristor structure is shown in Figure 3.a. The integrated circuit shown in Figure 3.b, which has 8 Tungsten-based Knowm memristors in a 16 pin ceramic DIP package, is used in this study. More information about Knowm memristors can be found in [38]. The pin connections of the memristors are given in Figure 3.c. Knowm memristors require using a series protection resistor to limit its current [38]. One of the Knowm memristors is placed in series with a protection resistor and excited with a sinusoidal signal as shown in Figure 4. A series resistor and a memristor also behave as a memristor as explained in [1]. The series resistor is used to measure the memristor current since its voltage and current are proportional. All of the operational Tungsten-based memristors are used in the experiments but only the results of one of them are given due to space considerations. Its current and voltage waveforms and its zero-crossing pinched hysteresis curves acquired for three different frequencies and are shown in Figures 5 and 6, respectively. It can be seen that with increasing frequency, the area of the hysteresis loop gets smaller in size which is a fingerprint of memristive systems [13]. The Tungsten-based Knowm memristor is also excited with a square wave and its current and voltage waveforms and hysteresis curves are shown in Figures 7 and 8, respectively.

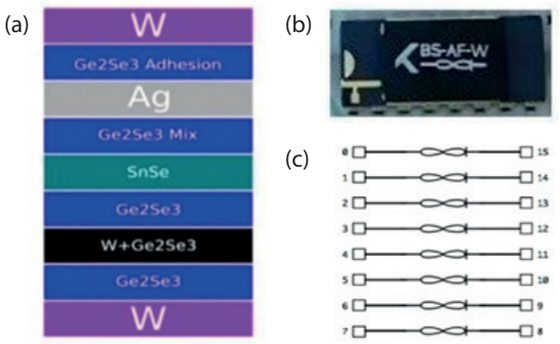

Figure 3: a) The Tungsten-based Knowm Memristor Topology [38], b) The SDC Tungsten(W)-based Knowm Memristor Integrated Circuit, and c) its pin connections [38].

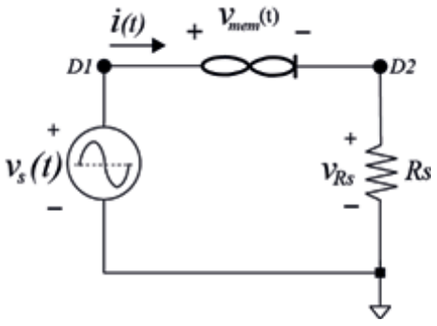

Figure 4: The Tungsten-based Knowm memristor excited with a signal source.

(a)

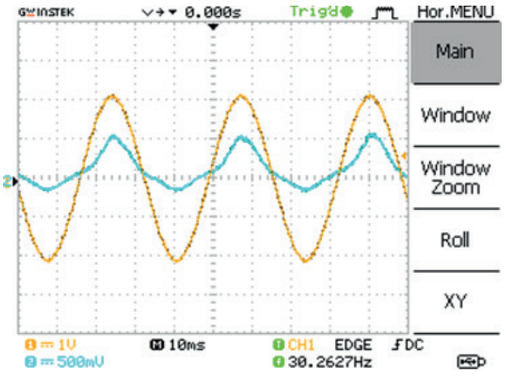

(b)

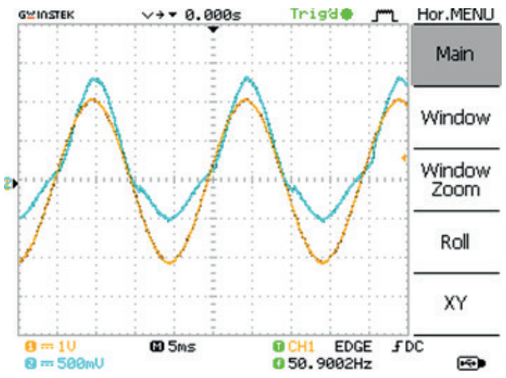

(c)

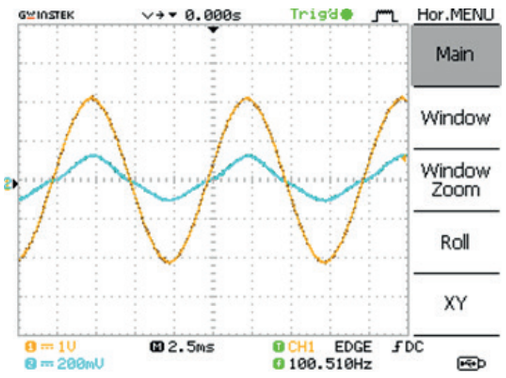

Figure 5: The time-dependent current and voltage waveforms of the Tungsten-based memristor fed with a a) 30, b) 50 Hz, and c) 100 Hz and a 2 V peak-to-peak sinusoidal voltage.

(a)

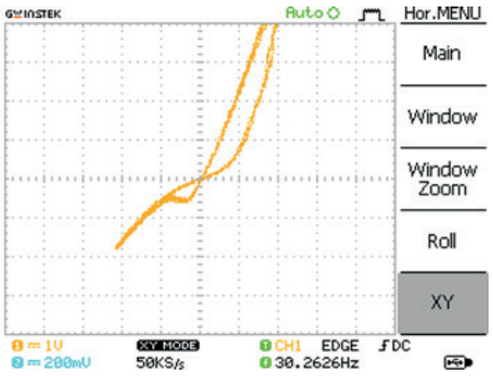

(b)

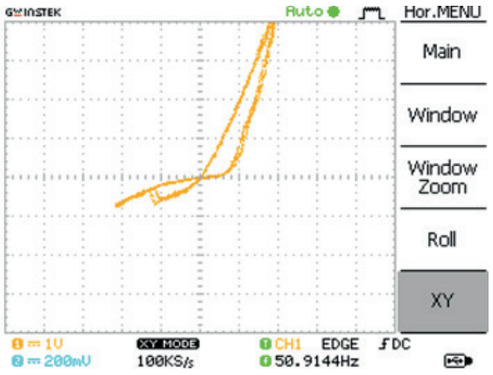

(c)

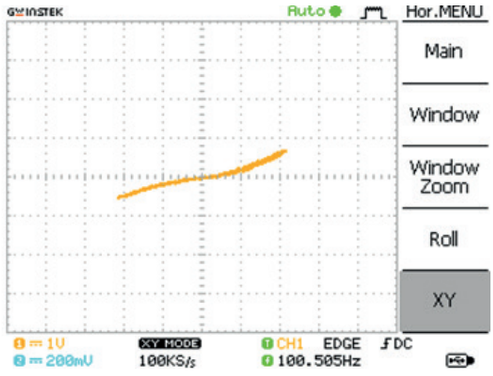

Figure 6: The hysteresis curve of the Tungsten-based memristor fed with a a) 30, b) 50 Hz, and c) 100 Hz and a 2 V peak-to-peak sinusoidal voltage.

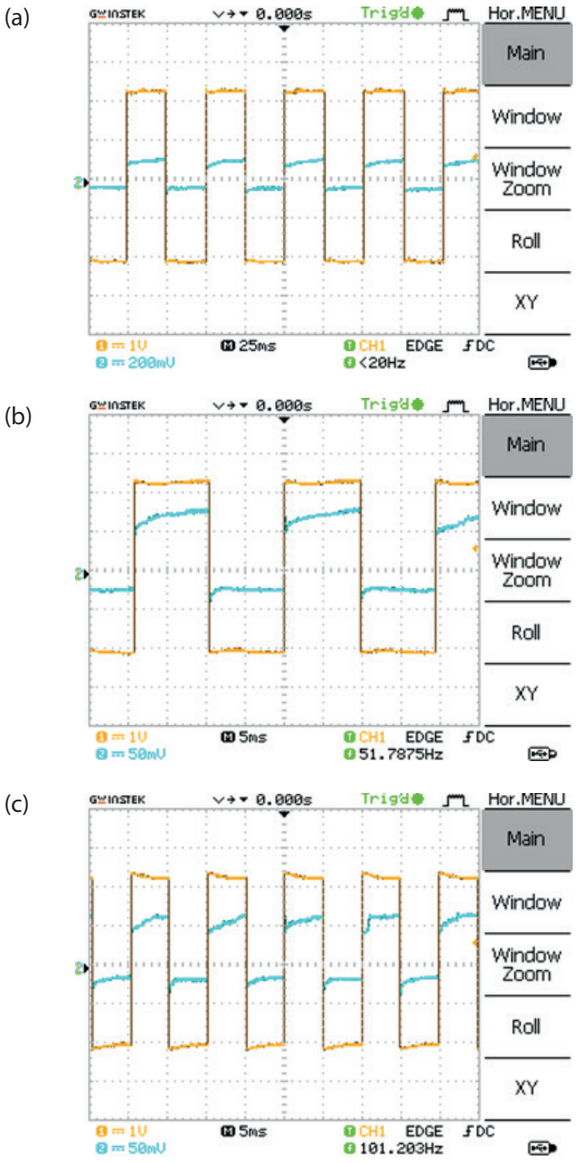

Figure 7: The time-dependent current and voltage waveforms of the Tungsten-based memristor fed with a a) 20 Hz, b) 50 Hz, c) 100 Hz and an approximately 2.4 V peak-to-peak square voltage.

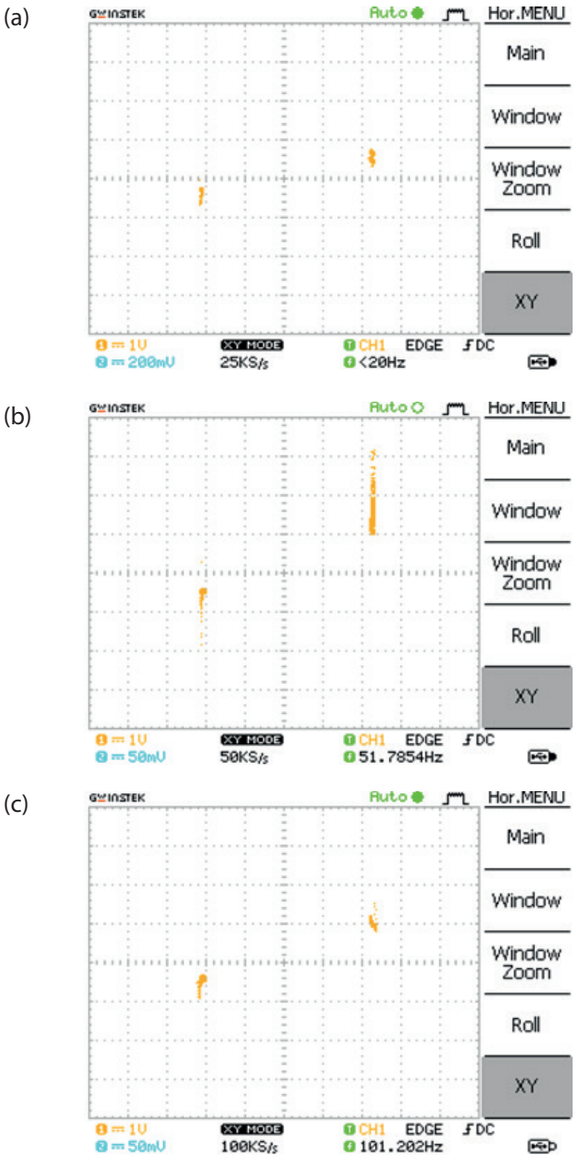

Figure 8: The hysteresis curve of the Tungsten-based memristor fed with a a) 20 Hz, b) 50 Hz, c) 100 Hz, and an approximately 2.4 V peak-to-peak square voltage.

4 Experiments

In this section, the experimental results of the Tungsten-based memristor-capacitor-protection resistor (M-C-R_s) series circuit shown in Figure 9 are given. A series protection resistor is used in all the experiments as suggested in [38] for protection and measuring the memristor current as shown in Figure 9. The circuit parameters are given in Table 1. With the M-C-R_s series circuit, the charging and discharging of the capacitor through the protection resistor and the memristor was investigated using an oscillator as a square wave voltage source and an oscilloscope. A square wave can be described as

$$V(t)=\begin{cases} V_p & , \quad 0<t<T/2 \\ -V_p & , \quad T/2<t<T \end{cases} \tag{14}$$

where V_p and T are the amplitude and the period of the square wave, respectively.

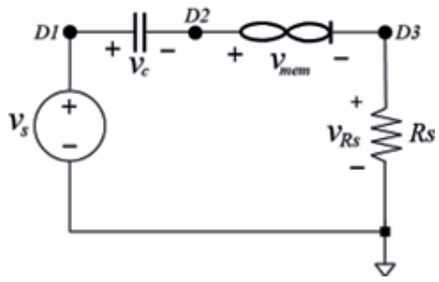

Figure 9: The Tungsten-based memristor-capacitor-protection resistor (M-C-R_s) series circuit excited with a square wave voltage source.

Table 1: The circuit parameters

Parameter	Value
C	200 nF
R_S	99.8 kΩ

The square wave is chosen due to having both polarities which makes the examination of the polarity-dependent charging possible. The experimental results are shown in Figure 10. It can be seen that the current of the Tungsten memristor becomes negative for a while when the Tungsten memristor voltage is positive or vice versa. Also, the circuit's charging behavior is not exponential.

As seen in Figure 10.a, at 2 Hz, the SDC Tungsten-based memristor current and the voltage at node D2 do not always have the same polarity. The current also goes negative when the voltage at node D2 is positive or vice versa. The negative maximum value of the device current gets is low compared to the positive maximum value. The current looks like a critically damped circuit current and has a bump at the bottom. At the beginning of the positive half period, the current is maximal, then, it falls down and becomes zero, it takes negative values after that, it becomes minimal, and then it starts increasing again. The polarity of the voltage at node D2 changes before the current becomes zero or changes its polarity again. A similar description can also be made for the negative half period. The memristor current and the voltage at node D2 do not have half wave symmetry.

As seen in Figure 10.b, at 5 Hz, the SDC Tungsten-based memristor current and the voltage at node D2 do not always have the same polarity. The current also goes negative when the voltage at node D2 is positive or vice versa. The negative maximum value the device current is low compared to the positive maximum value. The current looks like a critically damped circuit current and has a bump at the bottom. At the beginning of the positive half period, the current is maximal,

(a)

(b)

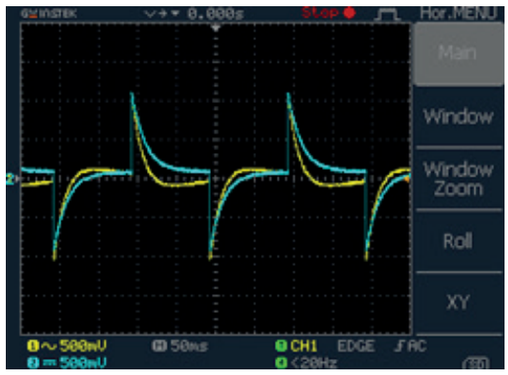

(c)

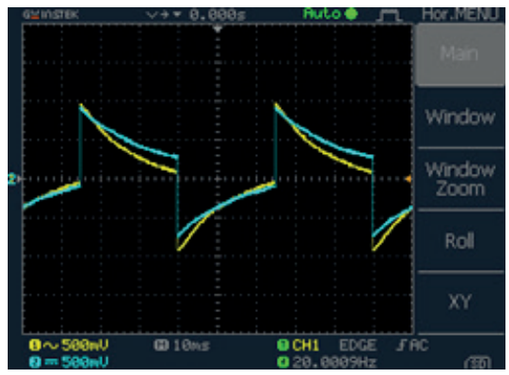

(d)

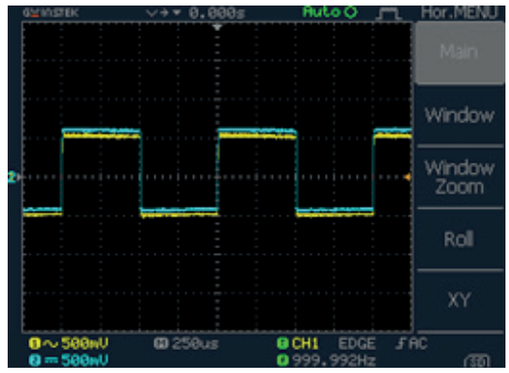

Figure 10: The current of the Tungsten-based memristor and the voltage waveform at node D2 when the M-C-R_s series circuit is fed with a a) 2 Hz, b) 5 Hz, c) 20 Hz, and d) 1 kHz, and a 2 V peak-to-peak square wave voltage.

it falls down, it becomes zero, it takes negative values, it becomes minimal, then it starts increasing again, and the polarity of the voltage at node D2 changes before the current becomes zero or changes its polarity again. A similar description can also be made for the negative half period. The current and the voltage at node D2 do not have half wave symmetry. The bump width seen in Figure 10.b is almost around the half period since the frequency of the signal is increased from 2 Hz to 5 Hz and its period is decreased.

As seen in Figure 10.c, at 20 Hz, the SDC Tungsten-based memristor current and voltage have the same polarity. The capacitive current also exists in this case. This can be explained by the fact that before the capacitive current component starts taking negative values, the polarity of the voltage changes. As seen in Figure 10.d, at a frequency high enough, at 1 kHz, in this case, the SDC Tungsten-based memristor starts behaving as a nonlinear resistor as described with one of the three fingerprints of a memristor.

Using MATLAB with the acquired data, the memristor current is calculated using Ohm's law:

$$i(t) = \frac{v_{R_S}(t)}{R_S} \tag{15}$$

The memristor current and voltage are shown in Figure 11. When excited with a sinusoidal or a square wave voltage source, the Tungsten-based SDC memristor has a zero-crossing curve as seen in Figures 6 and 8. However, when the M-C-R_s series circuit is excited with a square wave voltage source, the hysteresis curve of the memristor is not zero-crossing and its behavior is capacitive as seen in Figure 11. This phenomenon has not been reported in the literature or the datasheet until now [38]. More data on the polarity-dependent charging and discharging of capacitor circuits containing Tungsten- and Carbon-based Knowm memristors and using square waves and clock signals for forward and reverse polarities can be found in [48].

5 Discussions and model suggestions

The experimental waveforms show that a Tungsten-based SDC memristor is actually not a memristor and even not a memristive system due to lacking a zero-crossing hysteresis curve [2, 13]. Chua has described a memristor as a power-dissipating circuit component [4]. According to Chua, a memristor dissipates power and should not provide power. Also, the hysteresis of a memristor should only exist in the first and third quadrants [2, 13]. The Lissajous curves in Figure 12 show that the SDC Tungsten-based memristive system behaves as a nonlinear capacitive system since its hysteresis curves or v-i characteristics also exist in the second and the fourth quadrants where the system supplies power instead of consuming since, in the second and the fourth quadrants, its instantaneous power becomes negative:

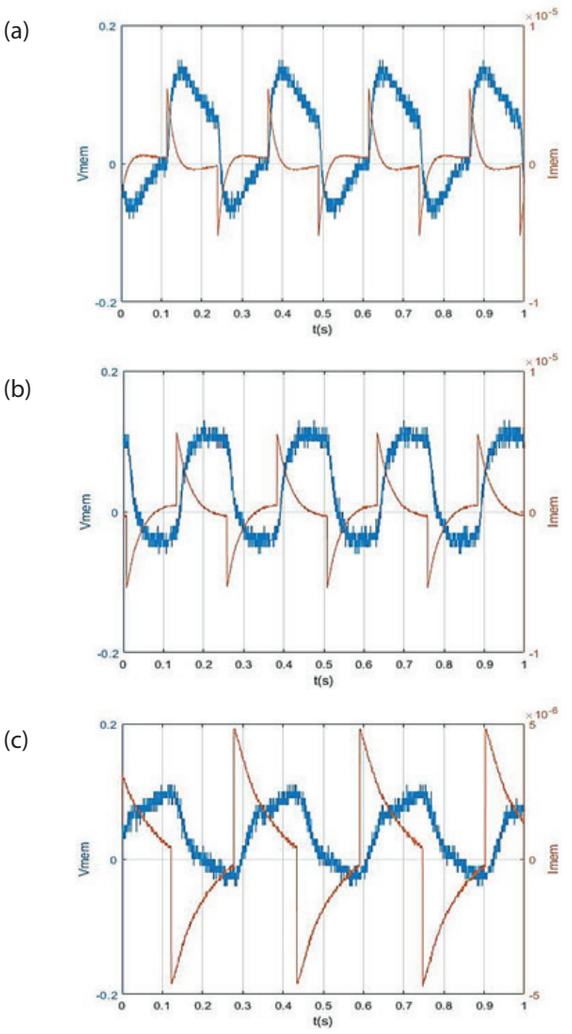

Figure 11: The time-dependent current and voltage waveforms of the Tungsten-based memristor when the M-C-R_s series circuit is fed with a a) 5 Hz, b) 10 Hz, and c) 20 Hz, and a 2 V peak-to-peak square wave voltage.

$$p(t) = v(t)i(t) < 0 \tag{16}$$

Its hysteresis curves are also in the second and fourth quadrants of the Cartesian coordinate system as shown in Figure 12.

(a)

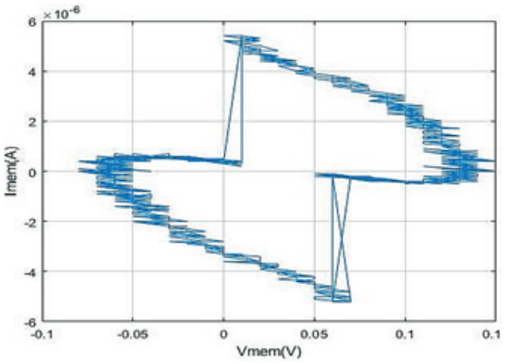

(b)

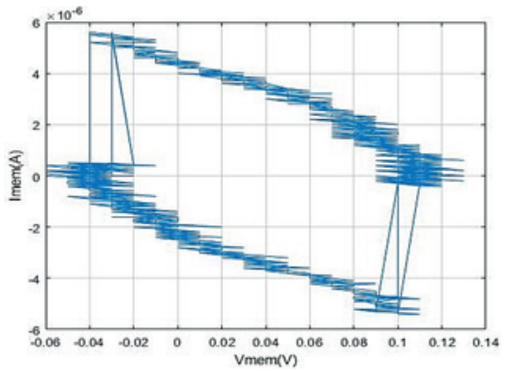

(c)

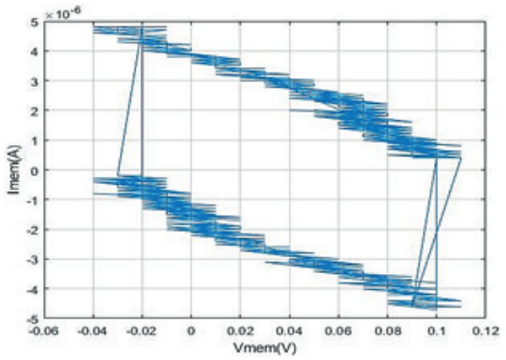

Figure 12: The hysteresis curve of the Tungsten-based memristor when the M-C-Rs series circuit is fed with a a) 5 Hz, b) 10 Hz, and c) 20 Hz, and a 2 V peak-to-peak square wave voltage.

The constitutive law of a capacitor is given as

$$i_c(t) = C\frac{dv_c(t)}{\mathrm{dt}} \tag{17}$$

A presumed current and voltage waveform of a capacitor is shown in Figure 13. The intervals where the derivatives of the memristor current are positive or negative have been marked in Figure 13. A capacitor current is positive when its voltage increases, or it charges and vice versa. If the derivative of the capacitor voltage is positive, its current is positive, and vice versa. Figure 13 is quite similar to the waveforms shown in Figure 11. However, there is a small shift at the point where the capacitor current becomes zero. This also means the memristive or resistive current component is quite low, compared to the capacitive current component. The Tungsten-based SDC memristor is actually a more complex system since it also shows a capacitive effect. Considering the voltages and currents shown in Figure 11, the Tungsten-based SDC memristor device has a capacitive behaviour. The current becomes negative even though the memristive behaviour does exist. We propose the following circuit model given in Figure 14 that explains all the phenomena. The model is made of a memristor and a memcapacitor connected in parallel.

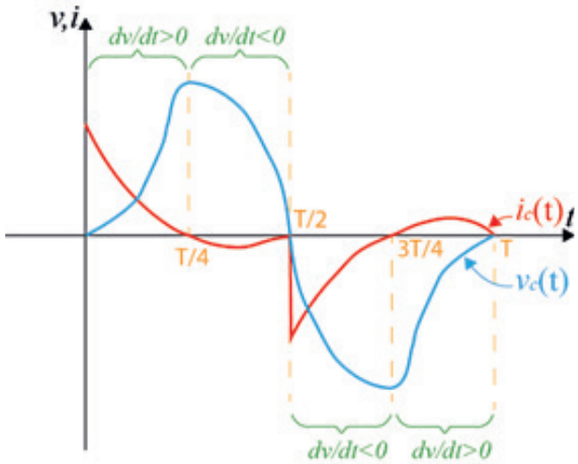

Figure 13: The representative capacitive behavior of the Tungsten memristor.

It should be examined where the capacitive current or the capacitance comes from. The simplest solution is to assume that the Schottky diode shown in the equivalent circuit given in Figure 2 has a capacitance. It is well-known that, assuming that Schottky barriers were formed at the top and bottom interfaces, the capacitance of a Schottky diode [49, 50] can be represented by:

$$C_m = \sqrt{\frac{q\varepsilon_i\ \varepsilon_0 N_D A^2}{2\left(\mathrm{V}_{bi} - V\right)}} \tag{18}$$

Where N_D is the donor density, ε_i is the relative permittivity of the interfacial layer, ε_0 is the permittivity of vacuum V_{bi}, is the built-in voltage, and V is the applied voltage.

The capacitance is dependent on the Schottky diode voltage. The lower the Schottky-diode voltage, the higher the Schottky-diode capacitance. More information on Schottky diode capacitance can be found in [49, 50]. As seen in Eq. (18), Schottky diode capacitance has

a nonlinear dependency on the Schottky diode voltage. Therefore, it is a nonlinear capacitance. The SDC Tungsten-based memristor topology and the Schottky diode topology in [49, 50] are not the same. That's why Eq. (19) cannot be used for calculation of the capacitance of the SDC Tungsten-based memristor but the Schottky diode capacitance of the SDC Tungsten-based memristor can still be assumed to be a nonlinear capacitance. A new equivalent circuit with it is given in Figure 14.a.

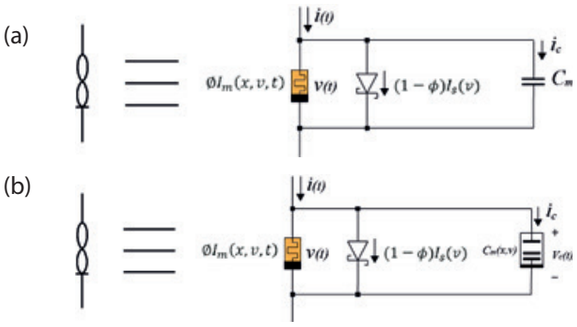

Figure 14: The new equivalent circuit of the Tungsten-based memristor a) with a nonlinear capacitor and b) a memcapacitor connected in parallel with the memristive element and the Schottky diode.

The threshold voltages of the SDC Tungsten-based memristor is given in Table 2. The forward threshold voltage of the SDC Tungsten-based memristor, ranges from 0.15 V to 0.35 V, and the reverse threshold voltage of the SDC Tungsten-based memristor, ranges from -0.27 V to -0.05 V according to [38]. Considering the voltage level of the SDC Tungsten-based memristor is less and around the threshold voltages in Figures 11 and 12, the capacitive effect may be higher if the voltage of the SDC Tungsten-based memristor is low or less than the threshold voltages.

Table 2: The threshold voltages of the SDC Tungsten-based memristor [38] W, Sn, C Types

Characteristic	Condition	Min	Typ	Max
Forward Threshold	DC/Quasi-static	0.15V	0.26V	0.35V
Reverse Threshold	DC/Quasi-static	-0.27V	-0.11V	-0.05V
Cycle Endurance	1.5Vpp, 500Hz sine wave, series resistor	50M	100M	5B

The existence of the polarity dependence of the memristor voltage and current can be seen in Figures 11 and 12. The current and voltage waveforms shown in Figure 11 also lack half-wave symmetry. The hysteresis curves are not symmetric with respect to origin as seen in Figure 12.

A Schottky diode capacitor's current is given as

$$i_c(t)=\frac{dq}{\mathrm{dt}}=\frac{dq}{\mathrm{d}v_c}\frac{dv_c(t)}{\mathrm{dt}}=C_m(v_c)\frac{dv_c(t)}{\mathrm{dt}}= \\ =C_m(v)\frac{dv(t)}{\mathrm{dt}} \tag{19}$$

where q is the Schottky diode charge.

The Schottky diode capacitance function, $C_m(v)$, is not written explicitly, and it requires further work to find its expression. The equation set describing the Tungsten-based memristor equivalent circuit with the nonlinear capacitor is given as

$$i(t)=\left(\frac{\phi x}{R_{ON}}+\frac{\phi(1-x)}{R_{OFF}}\right)v(t)+ \\ (1-\Phi)\alpha\left(e^{\beta_1 v(t)}-e^{-\beta_2 v(t)}\right)+ \\ +C_m(v)\frac{dv(t)}{\mathrm{dt}} \tag{20}$$

$$\frac{dx}{dt}=\frac{1}{\tau}\left(\frac{1}{1+e^{-\beta(v-V_{ON})}}(1-x)-\left(1-\frac{1}{1+e^{-\beta(v+V_{OFF})}}\right)x\right) \tag{21}$$

The Tungsten-based SDC memristor may be showing a memcapacitive effect. The Schottky diode capacitance may be dependent on the state variable of the Tungsten-based memristor, *x(t),* besides its voltage. In this case, it can be modeled as a memcapacitor as shown in Figure 14.b. If there is only one state variable, the current of a memcapacitive system can be given as

$$i_c(t)=\frac{dq_c(t)}{\mathrm{dt}}=\frac{d\left(C\left(x(t),v_c(t),t\right)v_c(t)\right)}{\mathrm{dt}}= \\ =\frac{\partial\left(C\left(x,\,v(t),\,t\right)\right)}{\partial \mathrm{x}}\frac{dx}{\mathrm{dt}}v_c(t)+ \\ +C\left(x(t),v_c(t),t\right)\frac{dv_c(t)}{\mathrm{dt}} \tag{22}$$

By substituting Eq. (21) to Eq. (22), its current turns into:

$$i_c(t)=\frac{\partial\left(C\left(x,\,v(t),\,t\right)\right)}{\partial \mathrm{x}}\left(\frac{(1-x)}{1+e^{-\beta(v-V_{ON})}}- \right. \\ \left.-\left(1-\frac{1}{1+e^{-\beta(v+V_{OFF})}}\right)x\right)\frac{v_c(t)}{\tau}+ \\ +C\left(x(t),v_c(t),t\right)\frac{dv_c(t)}{\mathrm{dt}} \tag{23}$$

As seen in Eq. (23), a memcapacitor is a more complex component than a nonlinear capacitor with only voltage dependence given in Eq. (19). Since a Knowm memristor is used with a protection resistor, the equivalent circuits given in in Figure 15.

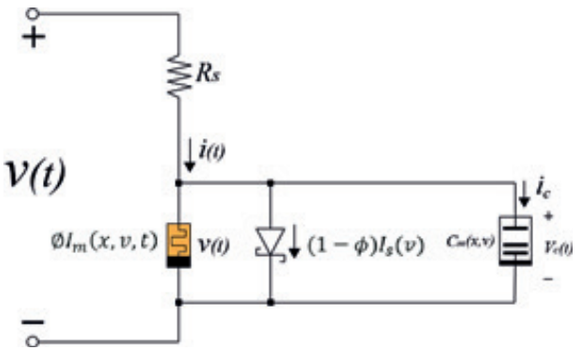

Figure 15: The equivalent circuit of the Tungsten-based Knowm Memristor.

The equation set describing the Tungsten-based memristor equivalent circuit with a memcapacitor and the series protection resistor can be given as

$$\begin{aligned} i(t) = &\left(\frac{\phi x}{R_{ON}} + \frac{\phi(1-x)}{R_{OFF}}\right) v_c(t) + \\ &+ (1-\Phi)\alpha\left(e^{\beta_1 v_c(t)} - e^{-\beta_2 v_c(t)}\right) + \\ &+ \frac{\partial\left(C\left(x,\, v(t),\, t\right)\right)}{\partial \mathrm{x}} \frac{dx}{\mathrm{dt}} v_c(t) + \\ &+ C\left(x, v_c(t), t\right) \frac{dv_c(t)}{\mathrm{dt}} \end{aligned} \tag{24}$$

$$\frac{dx}{dt} = \frac{1}{\tau}\left(\frac{1}{1+e^{-\beta(v_c - V_{ON})}}(1-x) - \left(1 - \frac{1}{1+e^{-\beta(v_c + V_{OFF})}}\right)x\right) \tag{25}$$

$$\frac{dv_c}{dt} = \frac{v(t) - v_c(t)}{R_s} \tag{26}$$

Eq. (26), the rate of change of the Tungsten voltage, is added to the Tungsten-based memristor system to distinguish Schottky diode charge and the memristive element charge, which are different or their state variables might be different or the Schottky diode memcapacitance might be dependent on two variables while the memristive element has only one state variable.

Mouttet has described memadmittance systems in [51]. Due to the existence of both the memristive and nonlinear capacitive or memcapacitive effects, the Tungsten-based memristor, in fact, must be called a Tungsten-based memadmittance system. Tungsten-based memadmittance system is abbreviated as (TBMS). The TBMS has actually richer dynamics than those described by Eq.s (10)-(11) as seen from Eq.s (24)-(26). The equations describing the behaviour of the chaotic circuits given in [39, 40] can also be modified or should be rewritten after finding a better model for the TBMS.

Since the the Tungsten-based memristor has a different topology than a Schottky diode, it is not obvious whether its capacitance is maximal at zero voltage. Under sinusoidal excitation, a zero-crossing hysteresis curve is possible as shown in Figure 6. Under square-wave excitation as shown in Figure 8, the hysteresis curve is in the first and the third quadrants, but the oscilloscope is unable to catch the curve passing through the origin. In our opinion, the capacitive current does also exist under square-wave excitation, but it needs further inspection why the hysteresis curve has zero crossing. Perhaps, it is not a zero-crossing curve, and the capacitive current component is much lower than the resistive current component, and the curve only looks like a zero-crossing hysteresis curve. If the device capacitance satisfies the following condition, the zero-crossing of the hysteresis curves becomes possible for both square and sinusoidal waves. If the device voltage *v(t)* = 0, the device capacitance is always zero:

$$C\left(x,0,t\right) = 0 \tag{27}$$

Therefore, when *v(t)* = 0, the capacitive current component of the device given by Eq. (22) turns into

$$i_c(t) = \frac{\partial\left(C\left(x,\, v(t),\, t\right)\right)}{\partial \mathrm{x}} \frac{dx}{\mathrm{dt}} 0 + C\left(x(t), 0, t\right) \frac{dv_c(t)}{\mathrm{dt}} = 0 \tag{28}$$

This causes the capacitive effect or the current of the capacitance of the system to vanish and a zero-crossing of the hysteresis curve to occur when the memristor voltage becomes zero. However, it should be examined whether this is true or not.

Due to having sufficiently high slopes, the waveforms in Figure 11 create a very high capacitive current large enough to make the device current become negative. This is not possible under square wave excitation since the square wave voltage has a very high slope while changing polarity but a zero slope after that.

If the capacitive current is much lower than the memristive current, its effect may not appear in the waveforms acquired and this may be the reason why the capacitive effects were not discovered and reported in the literature previously.

6 Conclusions

In this paper, the charging of the capacitor placed in series with a Tungsten-based memristor, and a resistor are examined experimentally by taking the polarity of the memristor into account. As a result of the experiments made:

- The charging of the capacitor is analyzed for both polarities of the memristor in the M-C-Rs series circuit. The charging of the M-C-R_s series circuit is found to be polarity dependent.
- In these experiments, it can be seen that the capacitor is not charged exponentially since the memristor current flows also in the opposite direction to the applied voltage for a while.
- In the literature review we conducted, it was seen that the Silver-Carbon-Silver (Ag-Carbon-Ag) topology was reported to behave as a system showing both memristive and memcapacitive effects without zero-crossing behavior [52]. We report that the tungsten-based memristor used in this study also exhibits capacitive or memcapacitive behavior.
- One of the findings of the paper is that "the SDC Tungsten-based Knowm Memristor" is not an ideal memristive system beside not being an ideal memristor.
- Another finding is that zero-crossing hysteresis curve and three fingerprints of a memristor is not always a signature of a memristive system, i.e., having the three fingerprints does not guarantee that it is a memristive system. All frequencies and voltage levels of a system must be considered. There may be a need for describing merged memristive and memcapacitive systems.
- It has been observed that the tungsten-based SDC memristor in the M-C-Rs circuit does not exhibit a considerable stochastic behavior as a Carbon-based SDC memristor does [48], but it behaves like a nonlinear R-C circuit at low frequencies and at the voltage levels examined.
- In this study, it has been found that Tungsten-based SDC memristor exhibit a capacitive behavior and a non-zero-crossing hysteresis curve. Therefore, it cannot be described only by the MMSMM model. Perhaps, the memcapacitive system equations, coupled with the equations of the MMSMM model can be used to model such a (memristive!) system. Here, we have suggested such a model without giving much detail. We suggest studying of the details of the memadmittance model as future work.
- The capacitance effects might be more dominant below threshold voltages and low frequencies.
- Since the MMSMM model, that does not include the capacitive effects, cannot accurately model the Tungsten-based memristors, the M-C-Rs series circuit cannot be analyzed using the MMSMM model.
- It is also true that the nonlinear dopant drift models [14-20] are not sufficient to model the Tungsten-based memristors since the models lack capacitive effects. Therefore, the M-C-Rs series circuit cannot be analyzed accurately using the nonlinear dopant drift models.
- As future work, the capacitive effects may be included using Shottky capacitance equation or modifying it to have a state variable dependency to include the memcapacitive effects. The behavior of the capacitance may be polarity dependent as shown in the experimental results section.
- Complete analysis of the M-C-Rs circuit can only be done after the Tungsten-based memristor is understood better and a more accurate Tungsten-based memadmitance model emerges.
- The Knowm memristor is shown to keep its state and its resistance can be tuned [38, 53]. This means that when its voltage is equal to zero its memristance value stays constant. If the condition given in Equation (27) is true and when the device voltage is zero, the memristor keeps its state. However, if the device capacitance is not zero when the device voltage is zero, this may result in information loss of the state of the device. Due to its importance, we also suggest this as future work.

More experimental data for M-C-Rs charging and discharging circuits with Tungsten- and Carbon-based Knowm memristors can be found in [48]. The resistive switching device measuring techniques are reviewed in [54], and it is implied that the parasitic capacitances existent in the test setup systems must also be considered and their effect on the measurements of the oxygen-ion-based ReRAMs must be minimized. Although SDC memristors belong to the metal-ion memristive systems, the same techniques suggested in [54] can be utilized to obtain better accuracy while acquiring the data to model their capacitive behavior by also considering the effect of the suggested protection resistor together with the parasitic capacitances on the device dynamics. This study can guide the researchers who will work in this direction in terms of methodology and experimental data. Tungsten-based Knowm memristors have complex structures [38]. Circuits such as programmable oscillators, comparators, and learning circuits [11] can be made with them. They need accurate models or more complex equivalent circuits perhaps involving memcapacitors to obtain the best performance from them.

7 Acknowledgment

This study was supported using the memristors bought by the project supported by the Scientific Research Projects Coordination Unit of Tekirdağ Namık Kemal University. Project number: NKUBAP.42.GA.19.206.

8 Conflict of interest

No conflict of interest was declared by the authors.

9 References

1. L. O. Chua, "Memristor-The Missing Circuit Element," IEEE Trans. Circuit Theory, vol. 18, pp. 507-519, 1971. https://doi.org/10.1109/TCT.1971.1083337
2. L. O. Chua, S. M. Kang, "Memristive devices and systems," Proc. IEEE, vol. 64, pp. 209-223, 1976. https://doi.org/10.1109/PROC.1976.10092
3. D. B. Strukov, G. S. Snider, D. R. Stewart, and R. S. Williams, "The missing memristor found," *Nature (London)*, vol. 453, pp. 80-83, 2008.
4. O. Kavehei, A. Iqbal, Y.S. Kim, K. Eshraghian, S.F. Al-Sarawi, and D. Derek, "The Fourth Element: Characteristics, Modelling, and Electromagnetic Theory of the Memristor," Proceedings of the Royal Society A: Mathematical, Physical and Engineering Sciences, vol. 466, pp. 2175-2202, 2010. https://doi.org/10.1098/rspa.2009.0553
5. T. Prodromakis, C. Toumazou, "A review on memristive devices and applications," 17th IEEE International Conference on Electronics, Circuits and Systems, 934-937, 2010. https://doi.org/10.1109/ICECS.2010.5724666
6. Y.V. Pershin, J. Martinez-Rincon, and M. Di Ventra, "Memory circuit elements: from systems to applications," Journal of Computational and Theoretical Nanoscience, 8(3), 441-448, 2011. https://doi.org/10.1166/jctn.2011.1708
7. Y. V. Pershin, M. Di Ventra, "Memory effects in complex materials and nanoscale systems," Adv. Phys., 60, 145–227, 2011. https://doi.org/10.1080/00018732.2010.544961
8. L. Chua, "Resistance switching memories are memristors," Applied Physics A, 102, 765–783, 2011. https://doi.org/10.1007/978-3-319-76375-0_6
9. R. Marani, G. Gelao, and A. G. Perri, "A review on memristor applications," International Journal of Advances in Engineering & Technology, 8(3), 294. 2015. https://doi.org/10.48550/arXiv.1506.06899
10. S. Sangho, K. Kim, and S. M. Kang, "Memristor applications for programmable analog ICs," IEEE Transactions on Nanotechnology, 10(2), 266-274, 2011. https://doi.org/10.1109/TNANO.2009.2038610
11. Y. Pershin, M. Di Ventra, "Practical Approach to Programmable Analog Circuits with Memristors," IEEE Transactions on Circuits and Systems I: Regular Papers, Vol. 57, p.p. 1857 – 1864, 2010. https://doi.org/10.1109/TCSI.2009.2038539
12. S. Vongehr, X. Meng, "The missing memristor has not been found", Scientific reports, 5(1), 11657, 2015. https://doi.org/10.1038/srep11657
13. S. P. Adhikari, M. P. Sah, H. Kim, and L. O. Chua, "Three fingerprints of memristor," IEEE Transactions on Circuits and Systems I: Regular Papers, vol. 60, no. 11, pp. 3008–3021, 2013, doi: 10.1109/TCSI.2013.2256171. https://doi.org/10.1007/978-3-319-76375-0_5
14. Y. N. Joglekar, S. J. Wolf. "The elusive memristor: properties of basic electrical circuits," European Journal of Physics 30.4, 661, 2009. https://doi.org/10.1088/0143-0807/30/4/001
15. Z. Biolek, D. Biolek, and V. Biolkova, "SPICE model of memristor with nonlinear dopant drift," Radio engineering, Vol. 18(2), pp. 210–214, 2009.
16. T. Prodromakis, B. P. Peh, C. Papavassiliou, and C. Toumazou, "A versatile memristor model with nonlinear dopant kinetics," IEEE transactions on electron devices, Vol. 58(9), pp. 3099-3105, 2011. https://doi.org/10.1109/TED.2011.2158004
17. J. Zha, H. Huang, and Y. Liu,"A novel window function for memristor model with application in programming analog circuits," IEEE Transactions on Circuits and Systems II: Express Briefs, Vol. 63(5), 423-427, 2016. https://doi.org/10.1109/TCSII.2015.2505959
18. Y. Oğuz, F. Gül, H. Eroğlu, "A New Window Function for Memristor Modeling," In 8th International Advanced Technologies Symposium (IATS17), pp. 3498-3502, 2017.
19. E. Karakulak, R. Mutlu, "SPICE Model of Current Polarity-Dependent Piecewise Linear Window Function for Memristors," Gazi University Journal of Science, 33(4), 766-777, 2020. https://doi.org/doi.org/10.35378/gujs.605118
20. R. Mutlu, T. Dabanoglu Kumru, "A Zeno Paradox: Some Well-known Nonlinear Dopant Drift Memristor Models have Infinite Resistive Switching Time," Radio Engineering, vol. 32, no. 3, pp. 312-324, 2023. https://doi.org/10.13164/re.2023.0312
21. M. Di Ventra, Yu. V. Pershin, and L. O. Chua "Circuit Elements with Memory: Memristors, memcapaci-

tors and meminductors," Proc. IEEE, vol. 97, pp. 1717–1724, 2009. https://doi.org/10.1109/JPROC.2009.2021077
22. E. Karakulak, R. Mutlu, "Explanation of Hysteresis Curve of a Fluxdependent Memcapacitor Memory capacitor Using Taylor Series and Parametric Functions," 6th International Advanced Technologies Symposium, IATS 11, 16.05.2011-18.05.2011.
23. D. Park, P. Yang, H. J. Kim, K. Beom, H. H. Lee, C. J. Kang, and T. S. Yoon, "Analog reversible nonvolatile memcapacitance in metal-oxide-semiconductor memcapacitor with ITO/HfOx/Si structure," Applied Physics Letters, 113(16), 162102, 2018. https://doi.org/10.1063/1.5043275
24. R. K. Singh, K. Mamta, "An account of spin memristive and memcapacitive systems: Next generation memory devices," *IOSR Journal of Applied Physics (IOSR-JAP) e-ISSN: 2278-4861,* vol. 6, no. 3, pp. 07-23, 2014.
25. J. Martinez-Rincon, M. Di Ventra, and Y. V. Pershin, "Solid-state memcapacitive system with negative and diverging capacitance," *Physical Review B*, vol. 81, no. 19, pp. 195430, 2010. https://doi.org/10.1103/PhysRevB.81.195430
26. M. Krems, Y. V. Pershin and M. Di Ventra, "Ionic Memcapacitive Effects in Nanopores," *Nano letters*, vol. 10, no. 7, pp. 2674-2678, 2010. https://doi.org/10.1021/nl1014734)
27. J. Flak, and J. K. Poikonen, "Solid-state memcapacitors and their applications," *In: Memristor Networks,* Springer, Cham, pp. 585-601, 2014. https://doi.org/10.1007/978-3-319-76375-0_43
28. Y. Shen, G. Wang, Y. Liang, S. Yu, and H. H. C. Iu, "Parasitic memcapacitor effects on HP TiO2 memristor dynamics", *IEEE Access,* vol. 7, pp. 59825-59831, 2019. https://doi.org/10.1109/ACCESS.2019.2914938
29. J. Sun, E. Lind, I. Maximov, H. Q. Xu, "Memristive and Memcapacitive Characteristics of a Au/Ti–HfO2-InP/InGaAs Diode," *Electron Device Letters, IEEE*, vol.32, no.2, pp.131-133, Feb. 2011. https://doi.org/10.1109/LED.2010.2090334
30. J. Martinez-Rincon, and Y. V. Pershin," Bistable nonvolatile elastic-membrane memcapacitor exhibiting a chaotic behavior," IEEE transactions on electron devices, vol. 58, no. 6, pp. 1809-1812, 2011. https://doi.org/10.1109/TED.2011.2126022
31. M. E. Fouda, and A. G. Radwan, "Resistive-less memcapacitor-based relaxation oscillator," International Journal of Circuit Theory and Applications, vol. 43, no. 7, pp. 959-965, 2015. https://doi.org/10.1002/cta.1984
32. Ş. Ç. Yener, R. Mutlu, "Small signal model of memcapacitor-inductor oscillation circuit," in Electric Electronics, Computer Science, Biomedical Engineerings' Meeting (EBBT), pp. 1-4, 2017. https://doi.org/10.1109/EBBT.2017.7956774
33. Z. Hu, Y. Li, L. Jia, and J. Yu, "Chaotic oscillator based on voltage-controlled memcapacitor," in International Conference on Communications, Circuits and Systems (ICCCAS), pp. 824-827, 2010. https://doi.org/10.1109/ICCCAS.2010.5581863
34. K. Rajagopal, A. Akgul, S. Jafari, and B. Aricioglu, "A chaotic memcapacitor oscillator with two unstable equilibriums and its fractional form with engineering applications," Nonlinear Dynamics, vol. 91, no. 2, pp. 957-974, 2018. https://doi.org/10.1007/s11071-017-3921-3)
35. F. Yuan, G. Wang, and X. Wang, "Chaotic oscillator containing memcapacitor and meminductor and its dimensionality reduction analysis," Chaos: An Interdisciplinary Journal of Nonlinear Science, vol. 27, no. 3, pp. 033103, 2017. https://doi.org/10.1063/1.4975825
36. F. Tulumbacı, Ş. Ç. Yener, R. Mutlu, "Stored Energy and the Charging Energy Efficiency in a Memcapacitor Circuit," in 6th International Conference on Electrical Engineering and Electronics, 2020. https://doi.org/10.11159/eee20.105
37. K. U. Demasius, A. Kirschen, and S. Parkin, "Energy-efficient memcapacitor devices for neuromorphic computing," Nature Electronics, vol.4, no.10, pp. 748-756, 2021. https://doi.org/10.1038/s41928-021-00649-y
38. Knowm, Self Directed Channel Memristors, Rev. 3.2, October 6, 2019, https://knowm.org/downloads/Knowm_Memristors.pdf. [accessed on July 2, 2023].
39. C. K. Volos, V. T. Pham, H. E. Nistazakis, I. N. Stouboulos, "A dream that has come true: Chaos from a nonlinear circuit with a real memristor," International Journal of Bifurcation and Chaos, 30(13), 2030036, 2020, https://doi.org/10.1142/S0218127420300360
40. L. Minati, L. V. Gambuzza, W. J. Thio, J. C. Sprott, and M. Frasca, "A chaotic circuit based on a physical memristor," Chaos Solitons Fractals, 138, 109990, 2020. https://doi.org/10.1016/j.chaos.2020.109990
41. M. A. Nugent, T. W. Molter, "AHaH Computing–From Metastable Switches to Attractors to Machine Learning," PLoS ONE, 9, e85175, 2014. https://doi.org/10.1371/journal.pone.0085175
42. C. Fernandez, A. Cirera, I. Vourkas, "Design Exploration of Threshold Logic in Memory and Experimental Implementation Using Knowm Memristors," Int. Journ of Unconventional Computing, Vol. 18, pp. 249–267, 2023.
43. The Mean Metastable Switch Memristor Model in Xyce. Available online: https://knowm.org/

the-mean-metastable-switchmemristor-model-in-xyce/ [accessed on 26 December 2021].
44. V. Ostrovskii, P. Fedoseev, Y. Bobrova, and D. Butusov, "Structural and parametric identification of knowm memristors," Nanomaterials, 12(1), 63, 2021. https://doi.org/10.3390/nano12010063
45. R. Mutlu, "Solution of TiO2 memristor-capacitor series circuit excited by a constant voltage source and its application to calculate operation frequency of a programmable TiO2 memristor-capacitor relaxation oscillator," Turkish Journal of Electrical Engineering & Computer Sciences, 23(5), pp. 1219-1229, 2015. https://doi.org/10.3906/elk-1108-38
46. N. N. Urgan, C. Dalmış, and R. Mutlu, "Analysis of the HP Memristor and Capacitor (M-C) Series Circuit Using the Lambert W Function," European J. Eng. App. Sci 3(2), 27-32, 2020.
47. M. A. Carrasco-Aguılar, F. E. Morales-López, C. Sánchez-López, R. Ochoa-Montiel, "Flux-charge analysis and experimental verification of a parallel memristor-capacitor circuit," Memories-Materials, Devices, Circuits and Systems, vol. 4, p. 1–6, 2023, https://doi.org/10.1016/j.memori.2023.100043
48. C. Dalmış, "Examination of polarity-dependent charging and discharging of capacitor circuits containing Carbon and Tungsten based memristors," Tekirdağ Namık Kemal University, Institute of Natural and Applied Sciences, Master's thesis, 2021. https://doi.org/10.1016/j.memori.2023.100043
49. S. M. Sze, "Physics of Semiconductor Devices 2nd ed." John Wiley & Sons, New York, 362-390, 1981.
50. F. Parlaktürk, A. Agasiev, A. Tataroğlu, and Ş. Altındal, "Current-Voltage (IV) and Capacitance-Voltage (CV) Characteristics of Au/Bi4Ti3O12/SnO2 Structures" Gazi University Journal of Science, 20(4), 97-102, 2007.
51. B. Mouttet, "A memadmittance systems model for thin film memory materials", arXiv preprint arXiv:1003.2842, 2010. https://doi.org/10.48550/arXiv.1003.2842
52. G. Zhou, Z. Ren, L. Wang, J. Wu, B. Sun, A. Zhou, G. Zhang, S. Zheng, S. Duan, and Q. Song, "Resistive switching memory integrated with amorphous carbon-based nanogenerators for self-powered device," Nano Energy 63, 103793, 2019. https://doi.org/10.1016/j.nanoen.2019.05.079
53. J. Gomez, I. Vourkas, A. Abusleme, G. C. Sirakoulis, and A. Rubio, "Voltage divider for self-limited analog state programing of memristors", IEEE Transactions on Circuits and Systems II: Express Briefs, 67(4), 620-624, 2019. https://doi.org/10.1109/TCSII.2019.2923716
54. A. Torrezan, G. Medeiros-Ribeiro, S. Tiedke, "Quasi-static and Pulse Measuring Techniques", Resistive Switching: From Fundamentals of Nanoionic Redox Processes to Memristive Device Applications, 341-362, 2016. https://doi.org/10.1002/9783527680870.ch12

Arrived: 20. 07. 2023
Accepted: 06. 11. 2023